04

Formation of the microchannel structure of a spark discharge in air in the gap spike-plane

© A.A. Tren'kin, K.I. Almazova, A.N. Belonogov, V.V. Borovkov, E.V. Gorelov, I.V. Morozov, S.Yu. Kharitonov

Russian Federal Nuclear Center, All-Russia Research Institute of Experimental Physics,
607190 Sarov, Russia
e-mail: alexey.trenkin@gmail.com

Received August 12, 2021
Revised November 25, 2021
Accepted November 26, 2021

The formation of the microchannel structure of a spark discharge in the gap spike (cathode)-plane of 1.5 mm length in the air of atmospheric pressure was studied by the method of shadow photography. The images with the concurrent descent of microchannel diameter sand the number of microchannel increase in the cathode region on the time interval of 5 ns were recorded. The obtained data are explained in the frames of the microstructure formation mechanism at the expense of the front instability of the ionization wave. The parameters characterizing the process of the microstructure formation are estimated, and they agree with the experimental data.

Keywords: spark discharge, ionization wave, ionization instability, microstructure, method of shadow photography.

DOI: 10.21883/TP.2022.03.53257.235-21

Introduction

The demand to practical applications of the electric discharges in dense gases stimulates the interest to study them in order to improve the efficiency of existing and development of new gas discharge technologies. Regardless of a long period of studies and high volume of the obtained data related to various aspects of gas discharge processes, a series of phenomena is still understudied. One of such phenomena is formation of the microstructure at the initial phase of discharges in the air of atmospheric pressure, when the channel is an aggregate of a high number of microchannels (filaments) [1–7]. Originally, the microstructure of a discharge was detected by the methods of autographs (imprints) on the surface of a plane electrode (see [5–7] and references in them). The microchannel structure within the volume of a discharge gap has been detected relatively recently with the use of laser probing and shadow and interference techniques based on it [1–4]. The complexity of experimental study of that phenomenon is determined by the need for provision of a high resolution spatial (micrometer level) and time (nano- and subnanosecond level) capacities of the diagnostics. Note that by using optical and electron-optical methods the microstructure was not possible to be resolved [1].

Along with that, the fact of availability of microstructure of the studied discharges is doubtless, while the issue of a mechanism of its formation still remains open.

One of possible causes of the discharge filamentation could be ionization-overheating instability, by the development of which we can explain, e.g., formation of multiple filamentary channels with the diameter from 60 to 100 μm in the initially homogeneous diffusion discharge in argon at the pressure of 300 Torr within the gap of spike–plane with the length of 3 mm [8]. However, formation of a microstructure there was registered 100–400 ns after the start of breakdown, versus the conditions of experiments [1–4], where microchannels are registered at the first nanoseconds after the breakdown. The estimates show that for such a short time development of ionization-overheating instability in the conditions of the experiments in question is unlikely [6].

More appropriate explanation is formation of filaments due to instability of the ionization wave front, which is indicated by a series of analytical-theoretical studies [6,7,9–13]. Along with that, there is no reliable experimental confirmation of that, which can be associated with the complexity of registration of the processes in the phase of the ionization wave propagation. Such a circumstance is conditioned by both the duration of that phase, and relatively low values of the concentration of electrons and gas density gradient at that moment, which does not allow to register the microstructure by the used methodologies [1–4].

The studies [1,2] dealt with the methodology of study of the spatial structure of discharge by the method of shadow photography with the spatial resolution 5 μm/3 pixel at the laser pulse duration at 50% of 6 ns. These studies recorded a microchannel structure of the spark discharge in the air of atmospheric pressure in the gap „spike–plane" at the initial stage of its development. It was ascertained that the channel is a bundle of a high number of microchannels. At the times from units to dozens of ns microchannels are developing and expanding from the spike into the depth of the discharge gap. Then, formation of common front of the cylindrical shock wave of the spark channel and its radial movement is observed. A significant disadvantage of this methodology was single-frame shooting that limited possibilities of the study of the discharge dynamics.

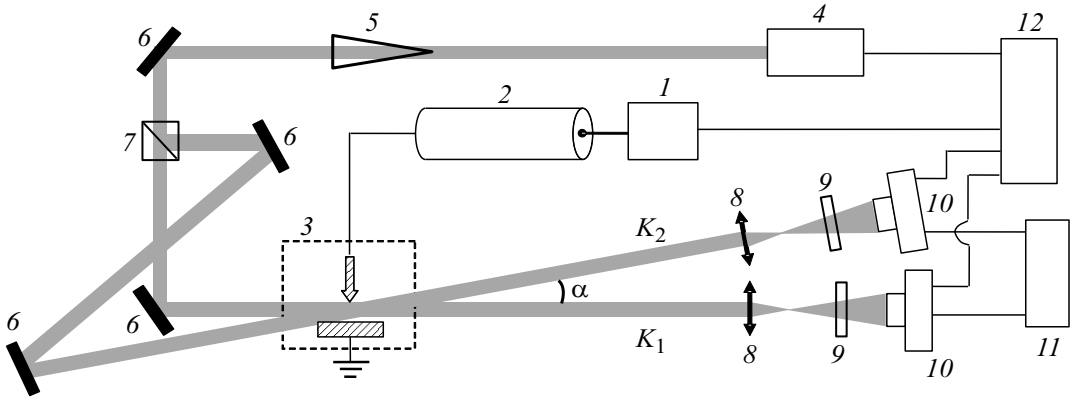

Figure 1. Block diagram of the experimental bench: *1* — pulsed voltage generator, *2* — cable line, *3* — discharge gap, *4* — probing radiation source (laser), *5* — collimator, *6* — swing mirror, *7* — light-dividing element, *8* — lenses, *9* — light filters, *10* — electron-optical recorder, *11* — personal computer, *12* — synchronization unit. Angle α between laser channels K_1 and K_2 is $\alpha = 15^\circ$.

This paper continues the studies [1,2]. Here, in evolution of the methodology of shadow photography, its double-frame shooting is implemented, which considerably expands the possibilities of obtainment the data on the processes accompanying gas discharges. The paper presents the results of study of a microstructure formation in a spark discharge.

1. Experimental setup and procedure

The diagram of the experimental bench is presented in Fig. 1. A part of its elements are characterized in detail in [1,2]. Pulsed voltage generator ensured negative polarity output pulse with an amplitude of 25 kV and a 0.1–0.9 rise time of approximately 7 ns. The pulse was applied to discharge gap through the cable line. Voltage and current measurements were performed at the pulsed voltage generator output by means of a capacitance divider and resistive shunt, accordingly. The temporal resolution of the divider and the shunt was less than 1 ns. Signals were recorded using an oscilloscope with a bandwidth of 500 MHz and a sample rate of 2 Gs/s.

The electrode system had a „spike–plane" geometry. An axially symmetric spike electrode is fabricated from stainless steel and had a length of 19 mm, diameter of 14 mm, an apex angle of 36°, and a curvature radius of 0.15 mm. A plane electrode was fabricated from an aluminum alloy and had the working part close in shape to a segment of a sphere with a diameter of 4.5 cm and a thickness of 1.5 cm. The interelectrode gap was 1.5 mm.

An optical detection system was used as a part of the bench. The system included a probing radiation source — solid-state laser (wavelength of 532 nm and a pulse duration at 50% of 6 ns), lenses, light filters, and digital electron-optical camera. A plane-parallel laser beam crossed the discharge region at a right angle to the spike–electrode axis and was detected by the electron-optical camera. The laser beam at the discharge generation region had a crosswise size of approximately 1 cm and a Gaussian profile. Since the interelectrode gap is far less than the bundle size, it ensured a homogeneous enough field of the laser radiation within the discharge region.

Shadow photography methodology is based on this system. These experiments, against those performed earlier [1,2], used double-beam optical scheme for the shadow methodology, thus ensuring obtainment of two frames per the pulse. Angle between the laser beams was approximately15°. The image in the discharge gap region was formed for each beam with a lens with a focal length of 23 cm at the photocathode of the electron-optical detector. The magnification coefficient is 10. The exposure of each frame was set by the laser pulse duration. The time interval between shadowgraph frames could be varied by altering optical path lengths of the beams. In the experiments the time interval was 5 ns. The frames were timed relative to the moment of breakdown, and the time characterizing them corresponds to the start of imaging.

Different stages of the discharge process were visualized by shifting the moments of actuation of the laser and the electron-optical detector relative to the moment of breakdown. The resolving power of the optical system was 5μm/3 pixel.

2. Experimental results and discussion

The discharge was studied in the air under normal conditions. An oscillatory process with exponential current and voltage decay was initiated in the discharge circuit after the breakdown of the gap. The oscillation period was 0.6 μs, and the amplitude and the decay time of current were 1 kA and 1.2 μs, respectively. At the same time, two characteristic moments were distinguished on oscillograms: occurrence of voltage within the discharge gap and breakdown. Average value of delay between them — 4 ns. The onset of the t_{bd} current rise (and the voltage decay) was assumed to be the moment of breakdown.

According to the results of studies performed earlier [1,2], the discharge dynamics at the initial phase seems to be the following. At the pre-breakdown stage a weakly

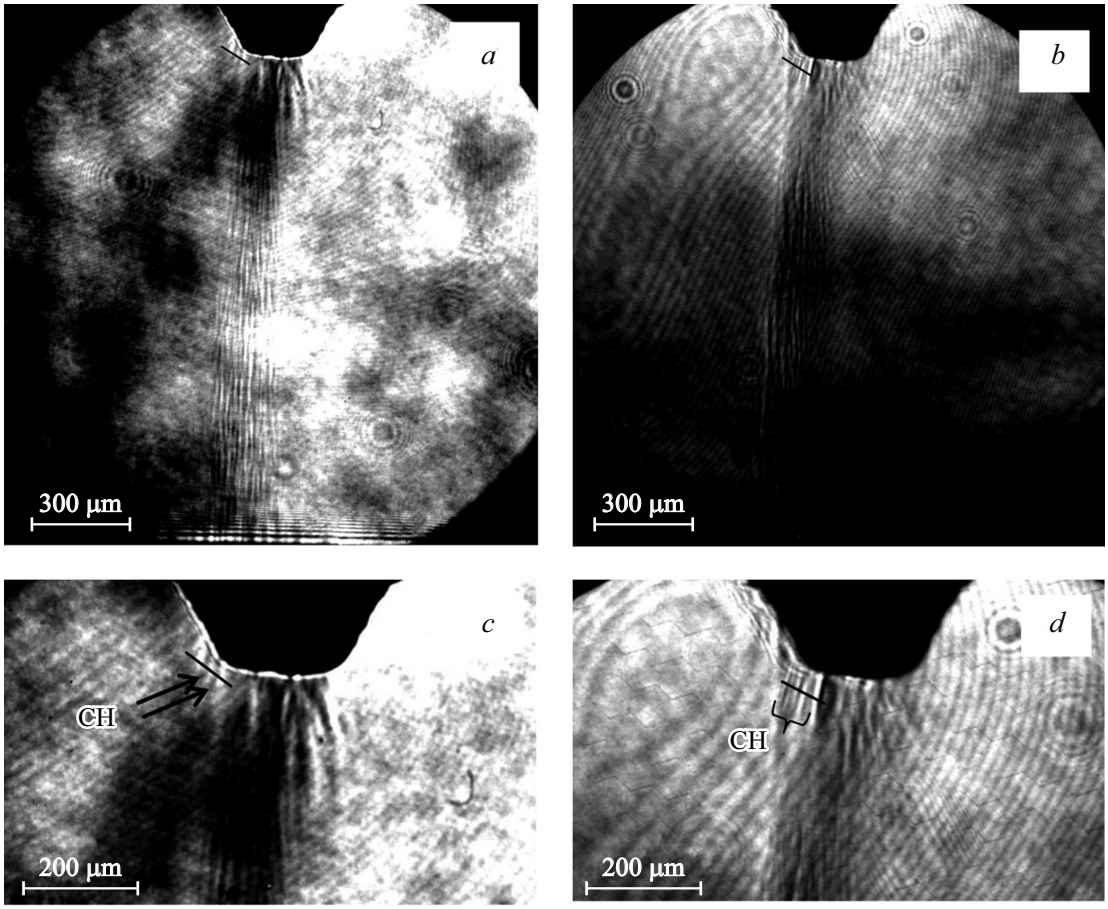

Figure 2. Shadowgraphs of the discharge in one pulse at the moment of time 9 (*a*) and 14 ns (*b*); *c* and *d* — relevant zoomed in fragments. Black line (*a, c* — the length 120 μm, *b, d* — 90 μm), crossing the channels CH, means the path along which the image value was built.

lighted diffusion channel and cathode spots appear, that begin formation of the spark channel. The channel has a microstructure, which is recorded on the shadowgraphs at the very first nanoseconds after breakdown. Until the moment of 15–20 ns the spark diameter remains virtually the same, the current is rising, and the electrons concentration at this moment reaches the maximum value, after which the channel expands radially with formation of cylindrical shock wave at its boundary.

The introduction mentioned a problem of recording the process of formation of the microstructure: high rates caused by significant overvoltage of the discharge gap in the pre-breakdown phase, and relatively low values of concentration of electrons and gas density gradients to be registered. However, after formation of the discharge channel, formation of delayed lateral channels, is often observed; the channels, originated from the cathode areas shifted from the axial region. In this phase the processes are developing at lower electrical fields, which causes their lower speed.

The obtained shadowgraphs (Fig. 2) detected the channels near to lateral surface of the spike electrode, that develop after formation of primary channel, and the use in these experiments of double-framing mode of shadow photography enabled registration of their dynamics.

There are two channels on the shadowgraph (Fig. 2, *a, c*) appearing as dark elongated areas. Black line (*a, c* — the length 120 μm, *b, d* — 90μm), crossing the channels CH, means the path along which the image value profile was built. Figure 3 presents this profile. The digits *1* and *2* refer to the characteristic minimums. Also, Fig. 3 shows profile of the image value in absence of the discharge. Comparison of two profiles shows that dark regions on the shadowgraph occur within the discharge itself, and not related to the peculiarities of the visualization field, which confirms their identification as the channels. Their diameters determined as FWHM 50% of the profile are 10–15 μm.

The shadowgraph (Fig. 2, *b, d*) obtained with the interval of 5 ns after the shadowgraph in Fig. 2, *a, c* detects several channels of lower diameter at the place of initial channels. Relevant profile of the image value is given in Fig. 4. The minimums that supposedly correspond to the channels are marked as digits from *1* to *4* in this figure. Based on the foregoing, one may assume that the number of channels is equal to four. It is noted the general image brightness fall in that region versus the image without discharge. Moreover,

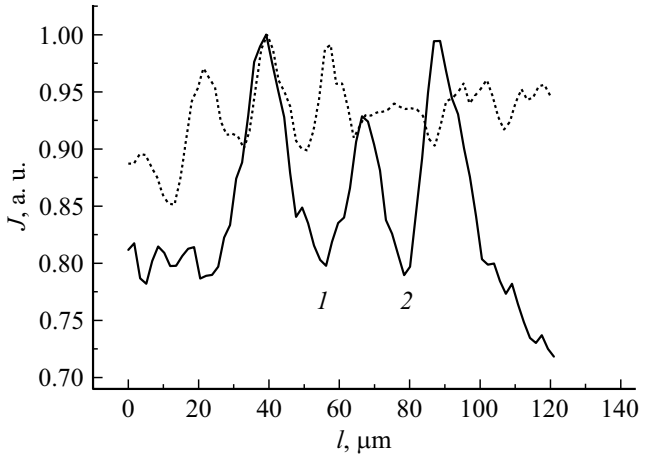

Figure 3. Image value profile J of the shadowgraph along the path l highlighted in Fig. 2, *a, c.* Dashed line — without discharge, solid line — with discharge.

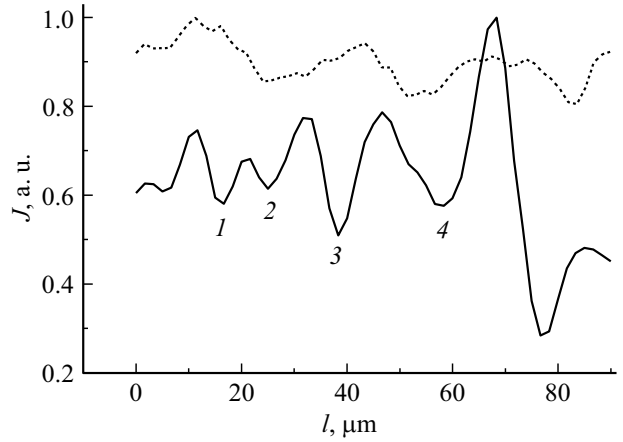

Figure 4. Image value profile J of the shadowgraph along the path l highlighted in Fig. 2, *b, d.* Dashed line — without discharge, solid line — with discharge.

the profile modulation is observed. Apparently, it is caused by partial overlapping of channels on the laser beam line. The channel diameters determined as above make from 5 to 10 μm, which is approximately two times less than the diameters of initial channels.

The found features of the gas discharge structure dynamics that include formation of channels with serial decrease of the diameter and increase of their number allow us to consider such a phenomenon as a result of the ionization front instability development. Relevant model of the mechanism of formation of the discharge microstructure was discussed earlier in [6,7]. Based on this model we make assessments for the conditions of these experiments, by assuming, that the channels registered on the shadowgraph of Fig. 2, *b, d* were formed as a result of the ionization instability of the front of channels presented in the shadowgraph of Fig 2, *a, c.*

By using the data on the sensitivity of the applied methodology, one may assume that concentration of electrons in the channels is at least $10^{16}\,\mathrm{cm}^{-3}$ [14]. Such a high value of concentration indicates that development of instability occurs not in the avalanche, but in the plasma phase [7]. For the conditions in question specific resistance of the channel plasma is $\rho \leq 1\,\Omega$ m, then the Maxwell's discharge relaxation time $\tau_M = \varepsilon_0 \rho \leq 10^{-11}$ s does not exceed characteristic time of the air ionization by electron impact $\tau_e \approx 10^{-11}$ s in the fields in question [15]. Such a circumstance allows to use approximation of the ideal conductivity of plasma for the process of our interest, and the assessment of time of the instability development at the channel head (ionization front) results as follows [9]:

$$t_{\mathrm{ins}} = \lambda/\mu E,$$

where λ is potential disturbance wavelength at the ionization front, μ is electrons mobility, E is electrical field strength. Assuming for our conditions $E = 100{-}300\,\mathrm{kV/cm}$, $\lambda = 10{-}20\,\mu$m, then $t_{\mathrm{ins}} \approx 10$ ps. Since t_{ins} of the order τ_e it can be assumed, that the size of forming channels l_m must be determined by the value of about α^{-1}, where α is the Townsend ionization coefficient. By using for α the formula [16]:

$$\alpha = Ap \exp(-Bp/E),$$

where p is the gas pressure, A and B are constants, for the conditions in question we obtain the value $l_m = 2{-}15\,\mu$m, that corresponds to the recorded values.

Therefore, the results obtained herein contribute into confirmation of the discharge microchannel structure formation mechanism due to the ionization front instability development.

Conclusion

With the use of the double-framing methodology of the shadow photography we studied the spark discharge in a gap „spike (cathode)−plane" with the length of 1.5 mm in the air of atmospheric pressure.

The performed studies have confirmed the data obtained earlier by means of the single-frame methodology, as to the discharge dynamics at the time moments from the breakdown to 100 ns, including: development of microchannels from the spike into the depth of the discharge gap, expansion of microchannels, formation of common spark channel front, cylindrical shock wave and its radial movement.

The dynamics of development of lateral channels in the near-to-cathode region was recorded within the time range from 9 to 14 ns, including serial formation of the lower diameter channels and the growth of their number. The diameter of the initial channel is $10{-}15\,\mu$m, the diameter of further channels — $5{-}10\,\mu$m, at the same time, the number of channels is doubled at the time scale that does not exceed 5 ns.

The obtained experimental data confirm the assumption on the mechanism of the microchannel structure formation due to instability of the ionization front. The assessments of

parameters characterizing the process of the microstructure formation were made, that correlate with the experimental data and provided assumption.

Conflict of interest

The authors declare that they have no conflict of interest.

References

[1] A.A. Trenkin, K.I. Almazova, A.N. Belonogov, V.V. Borovkov, E.V. Gorelov, I.V. Morozov, S.Yu. Kharitonov. Tech. Phys., **63** (6), 801 (2018). DOI: 10.1134/S1063784218060026
[2] A.A. Trenkin, K.I. Almazova, A.N. Belonogov, V.V. Borovkov, E.V. Gorelov, I.V. Morozov, S.Yu. Kharitonov. Tech. Phys., **65** (12), 1948 (2020). DOI: 10.1134/S1063784220120270
[3] E.V. Parkevich, M.A. Medvedev, A.I. Khirianova, G.V. Ivanenkov, A.S. Selyukov, A.V. Agafonov, K.V. Shpakov, A.V. Oginov. Plasma Sources Sci. Technol., **28**, 125007 (2019). DOI: 10.1088/1361-6595/ab518e
[4] E.V. Parkevich, M.A. Medvedev, G.V. Ivanenkov, A.I. Khirianova, A.S. Selyukov, A.V. Agafonov, Ph.A. Korneev, S.Y. Gus'kov, A.R. Mingaleev. Plasma Sources Sci. Technol., **28**, 095003 (2019). DOI: 10.1088/1361-6595/ab3768
[5] A.G. Rep'ev, P.B. Repin, V.S. Pokrovski'. Tech. Phys., **52** (1), 52 (2007).
[6] A.A. Trenkin, V.I. Karelin. Tech. Phys., **53** (3), 314 (2008). DOI: 10.1134/S1063784208030055
[7] V.I. Karelin, A.A. Trenkin. Tech. Phys., **53** (9), 1236 (2008). DOI: 10.1134/S106378420809017X
[8] Yu.I. Bychkov, F.I. Suslov, K.A. Tinchurin, A.G. Yastremskiy. FP, **17** (2), 196 (1991) (in Russian).
[9] E.D. Lozanskiy, O.B. Firsov. *Teoriya iskry* (Atomizdat, M., 1975) (in Russian).
[10] O.A. Sinkevich. TVT, **41** (5), 695 (2003) (in Russian).
[11] M. Arrayas, M. Fontelos, J. Trueba. Phys. Rev. Lett., **95** (5), 165001 (2005). DOI: 10.1103/PhysRevLett.95.165001
[12] A. Rocco, U. Ebert, W. Hundsdorfer. Phys. Rev. E, **66**, 035102(R) (2002). DOI: 10.1103/PhysRevE.66.035102
[13] A. Luque, F. Brau, U. Eber. Phys. Rev. E, **78**, 016206 (2008). DOI: 10.1103/PhysRevE.78.016206
[14] A.A. Trenkin, K.I. Almazova, A.N. Belonogov, V.V. Borovkov, E.V. Gorelov, I.V. Morozov, S.Yu. Kharitonov. Tech. Phys., **66** (2), 243 (2021). DOI: 10.1134/S1063784221020225
[15] E.M. Bazelyan, Yu.P. Raizer. *Fizika molnii i molniezashchity* (Fizmatlit, M., 2001), ISBN 5-9221-0082-3 (in Russian).
[16] Yu.P. Raiser. *Physics of Gas Discharge* (Intelligence, Dolgoprudny, 2009)